IEEE Access
Multidisciplinary | Rapid Review | Open Access Journal

Received October 26, 2017, accepted December 12, 2017, date of publication December 27, 2017,
date of current version February 14, 2018.

Digital Object Identifier 10.1109/ACCESS.2017.2785393

k-Coverage Estimation Problem in Heterogeneous Camera Sensor Networks With Boundary Deployment

ZHIMIN LIU[1] AND ZHANGDONG OUYANG[2]
[1]College of Computer and Information Engineering, Hunan University of Commerce, Changsha 410205, China
[2]School of Mathematics and Computational Science, Hunan First Normal University, Changsha 410002, China

Corresponding author: Zhangdong Ouyang (oymath@163.com)

This work was supported in part by the National Natural Science Foundation of China under Grant 11301169 and in part by the Key Laboratory of Hunan Province for New Retail Virtual Reality Technology under grant 2017TP1026.

ABSTRACT Coverage estimation is one of the fundamental issues of camera sensor networks (CSNs), and is also an important metric used to evaluate the monitoring quality of field of interest (FoI). In comparison with conventional omnidirectional sensor networks, coverage estimation in CSNs is more challenging due to the sensing region of camera sensor that is a sector-disk region. Moreover, the heterogeneous deployment of CSNs makes the coverage estimation problem even more complex. Currently, most of the literatures assume that a great number of camera sensors are directly deployed in the FoI. This paper assumes that all heterogeneous camera sensors are stochastically deployed outside the FoI. For such heterogeneous CSNs, we derived a k-coverage probabilistic expression to estimate the minimum number of camera sensors required for a desired level of k-coverage. To evaluate the performance of the proposed k-coverage estimation expression, several simulation experiments are conducted to validate the theoretical results.

INDEX TERMS Camera sensor networks, boundary deployment, k-coverage, node prediction.

I. INTRODUCTION

Recently due to the extensive applications of CSNs in agricultural monitoring, traffic surveillance, river monitoring etc, it has attracted many scholars to engage in related research [1]. Unlike conventional omnidirectional sensor networks, a typical camera sensor network consists of a large number of orientable and sector-disk camera sensors can perform monitoring tasks on the FoI to gather more detailed image information by uniform and dense deployment of camera sensors. However, in some actual application scenarios, such as channel water monitoring, railway track monitoring, country security etc [2]–[4], the FoI is inaccessible or difficult to deploy camera sensors directly, camera sensors can not be directly scattered inside the FoI, and only be deployed outside the FoI. Due to a great number of camera sensors are scattered in the boundary regions of the FoI, the existing studies on k-coverage problem in CSNs can not be directly applied to such scenarios.

Coverage estimation is one of the fundamental issues of CSNs, including estimate the minimum number of camera sensors needed to maintain a certain k-coverage. At present, a lot of research works mainly focus on the coverage estimation of stochastic deployed omnidirectional sensor networks. Wan et al. [5] analyzed the effect of sensing radius and sensor scale on the k-coverage rate for stochastically deployed omnidirectional sensor network, and the boundary effect was taken into account. Brass et al. [6] studied the coverage estimation problem with Boolean sensing model for either stationary or mobile sensors and targets under random deployment. Li et al. [7] presented a distributed self-location estimation expression based on Voronoi diagram to achieve k-coverage in omnidirectional sensor networks with mobile sensors. Aiming at coverage and connectivity prediction problem of WSNs, Xing et al. [8] proposed a square-based coverage and connectivity probability model used to calculate the minimum number of sensors that need to be deployed for maintaining a certain coverage and connectivity rate. By consideration of such application scenario that all sensors are randomly deployed outside the FoI to be monitored in omnidirectional sensor networks.

Coverage estimation in CSNs is more challenging due to the directional sensing characteristic of camera sensors. Currently, most of literatures assume that a large amount of camera sensors are stochastically deployed inside the FoI.

Zhao et al. [9] studied the coverage estimation based on different sensing model in directional sensor networks, aiming to such application scenario in which all sensors are randomly deployed inside a square rectangle monitoring region, the coverage probability model of each point in the monitoring region covered by at least one sensor is proposed, but the boundary effect and the k-coverage ($k \geq 2$) estimation model are not considered. In order to take full account of the boundary effect in DSNs, literature [10] taken analysis of the coverage estimation problem and presented a probability-based coverage estimation expression. Authors [11] studied the coverage estimation problem in rectangle region with deployment of heterogenous CSNs, and derived the closed-form solution for the coverage estimation by investigating into a new target detection model. To obtain more extensive coverage monitoring information, Wang et al. [12] first proposed the definition of full-view coverage, and also derived a sufficient condition on the sensor density needed for a level of full-view coverage in a random deployment CSNs. He et al. [13] conducted research on the full-view area coverage with minimum sensors in CSNs and proved that the full-view area coverage can be transformed into full-view target coverage. Moreover, authors proposed a greedy-based algorithm to minimize the number of camera sensors to guarantee the full-view coverage of a given region. Aiming at barrier coverage in CSNs, Literature [14] proposed a novel concept of local face-view barrier coverage, derived a rigorous probability bound for intruder detection for local face-view barrier coverage vis a feasible deployment pattern. Hu et al. [15] analyzed the static and mobile random deployed camera sensor networks, and derived the critical sensing radius for full view coverage under static model, 2-dimensional random walk mobility. To deploy a heterogeneous DSN with satisfied coverage requirement and network connectivity under the minimum cost constraint, authors [16] presented three algorithms (a greedy heuristic, local search, and particle swarm optimization) to solve it approximately. For the coverage enhancement problem in heterogeneous DSNs, two enhanced deployment algorithms (EDA-I and EDA-II) are presented to obtain high sensing coverage ratio in the bounded monitoring region [17].

In this paper, we consider a deployment scenario where heterogeneous camera sensors are stochastically scattered outside the FoI to be monitored. Among those existing literatures [10], [11] are most relevant to our work. However, the existing works, that focus on such scenario where all camera sensors are randomly deployed inside the FoI, can not be directly applied to estimate the effective camera sensors with minimum sensor density in our studied application scenario. To the best of our knowledge, there is no relevant study on estimating sensor density in such heterogeneous CSNs with boundary deployment.The main contributions of this paper are summarized as follows.

- We make analysis of k-coverage estimation in heterogeneous camera sensor networks with boundary deployment
- We use the notion of effective possible sensing region to derive an expression for the expectation area of the FoI that is k-coverage.
- We demonstrate the estimation expression of the minimum heterogeneous camera sensors required to achieve a certain k-coverage.

The rest of this paper is organized as follows. In section 2, the application deployment scenario and related definitions are given. Section 3 derives the expression for k-coverage estimation. A series of simulation results are given in Section 4. Section 5 is the conclusion.

II. DEPLOYMENT SCENARIO AND DEFINITIONS

A. DEPLOYMENT SCENARIO

In this paper, we assume that different types of heterogeneous camera sensors are randomly deployed in the outside region of the FoI. As shown in Fig.1, the shadow rectangle region, denoted as ψ, is the field of interest (FoI). The width of the FoI is denoted as ω; and the length of the FoI is denoted as L; the outside region of the FoI, denoted as Ω, is called boundary region in this paper, and its length and width, denoted as L and b, respectively.

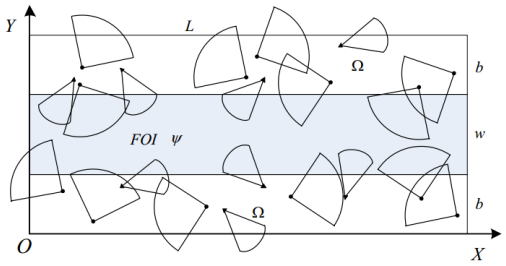

FIGURE 1. Illustration of heterogeneous camera sensors randomly deployed in the boundary region Ω to monitor FoI ψ.

B. SENSING MODEL

We use a 4-tuple $< s, \gamma, \alpha, \overrightarrow{f} >$ to denote the sensing model of camera sensor. As shown in Fig.2, where s, γ and α represent the camera sensor's position, sensing radius and field-of-view (Fov) respectively. The orientation of the camera sensor is denoted as $\overrightarrow{f}$. The sector-disk determined by $< s, \gamma, \alpha, \overrightarrow{f} >$ is defined as sensing region, denoted as $\|s\|$.

C. POSSIBLE SENSING REGION

The entire disk region that can be monitored by adjusting the orientation of camera sensor is called possible sensing region, denoted as $\phi(s)$. As shown in Fig.2.

D. EFFECTIVE POSSIBLE SENSING REGION

The possible sensing region of a camera sensor interacts with the FoI ψ is defined as effective probable sensing region, denoted as $\Phi = \phi(s) \cap \psi$, as shown in Fig.3.

E. DEFINITIONS

In this section, a grid model is adopted to calculate k-coverage rate of FoI.Fig.4 shows that the FoI is divided into I-row

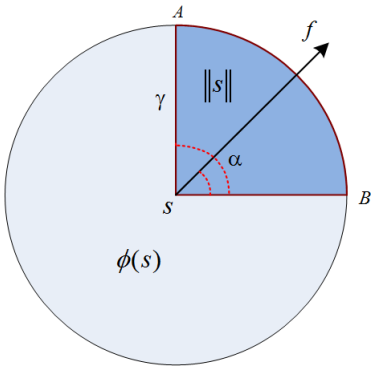

FIGURE 2. Illustration of sensing model and possible sensing region of camera sensor.

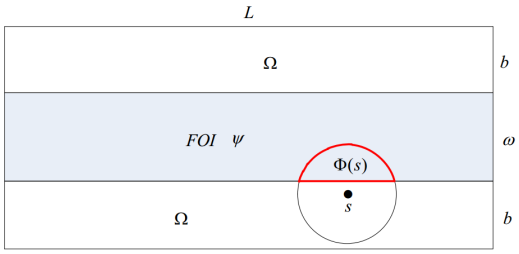

FIGURE 3. Illustration of sensing model and possible sensing region of camera sensor.

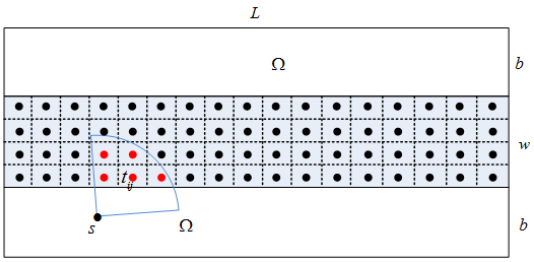

FIGURE 4. Illustration of grid division of the FoI ψ.

and J-column, respectively, so the FoI is divided into $I \times J$ partitions.The center point of each grid is regarded as its corresponding grid's position, the position of a grid point t_{ij} located in i-row-j-column is denoted as $(x_{t_{ij}}, y_{t_{ij}})$,where, $x_{t_{ij}} = \frac{L}{2I} + (i-1)\frac{L}{I}, y_{t_{ij}} = b + \frac{w}{2J} + (j-1)\frac{w}{J}, i = 1, ..., I, j = 1, ..., J$.

1) k-COVERED

As shown in Fig.4, for any grid in the FoI, denoted as $t \in \psi$. If the grid t falls within the sensing region of at least k camera sensors, the grid t is said to be k-Covered. The numerical k is called coverage degree.

2) k-COVERAGE RATE

The k-Coverage Rate is defined to be the percentage of grids in the FoI that are k-covered, it is denoted as $\mathbb{P} = \frac{G_k}{I \times J}$, where,$G_k$ represents the number of k-covered grids in the FoI, $I \times J$ represents the total number of grids in the FoI.

3) COMPLETE k-COVERED AND APPROXIMATELY COMPLETE k-COVERED

If the k-Coverage Rate is equal to 1, $\mathbb{P} = 1$, the FoI is said to be Complete k-Covered. If the k-Coverage Rate $\mathbb{P}$ is approximately equal to 1, the FoI is said to be Approximately Complete k-Covered.

F. MAIN NOTATIONS

To better describe the problem, the main notations in this paper are summarized as shown in Table 1.

TABLE 1. Description of notations.

Notation	Description
ψ	Field of interest, FoI
L	Length of FoI
ω	Width of FoI
Ω	Boundary region
b	Width of boundary region
s	Camera sensor
N	Scale of camera sensors
γ	Sensing radius
α	Field of view, FoV
$\|\|s\|\|$	Sensing region
$\phi(s)$	Possible sensing region
$\Phi(s)$	Effective possible sensing region
$E(\Phi)$	Expectation of effective possible sensing region
$\mathbb{P}$	k-Coverage Rate of the FoI

III. k-COVERAGE ESTIMATION IN HETEROGENEOUS CSNS

It can be seen from literature [18] that the distribution of a large number of sensors deployed in a region can be approximated as Poisson Distribution Process with sensor density λ. In heterogeneous CSNs, for simplicity, it is assumed that two different types of camera sensors called Type I and Type II are deployed in region R with different camera sensor density λ_1 and λ_2, sensing radius γ_1 and γ_2, field of view α_1 and α_2, respectively. A grid point t in the FoI said to be exactly covered by one camera sensor depends on two independent factors, that is, at least one camera sensor is located in a detection region D with radius γ centered at the grid point t and exactly one camera sensor is faced towards the grid point t. For different heterogeneous camera sensors, these have different detection regions(D_1 and D_2) with the same grid point t. It is derived that the probability of the grid point t which is covered by exactly k camera sensors in heterogeneous CSNs can be expressed as follow.

$$P(k) = \sum_{j=k}^{\infty} \sum_{i=0}^{j} \sum_{h=0}^{k} p(i; \lambda_1 \times D_1) C_i^h {q_1}^h (1-q_1)^{i-h} \times p(j-i; \lambda_2 \times D_2) C_{j-i}^{k-h} {q_2}^{k-h} (1-q_2)^{(j-i-k+h)} \quad (1)$$

Where, j represents the total number of Type I and Type II camera sensors in the detection regions D_1 and D_2 corresponding to the grid point t; h denotes that there are h Type I

camera sensor cover the grid point t; $p(i;\lambda_1 \times D_1)$ indicates the probability that the D_1 contains exactly i Type I camera sensors, that is, $p(i;\lambda_1 \times D_1) = \exp(-\lambda_1 \times D_1)\frac{(\lambda_1 \times D_1)^i}{i!}$. Similarly, $p(j-i;\lambda_2 \times D_2)$ denotes the probability that the detection region D_2 includes exactly $j-i$ Type II camera sensors, that is, $p(j-i;\lambda_2 \times D_2) = \exp(-\lambda_2 \times D_2)\frac{(\lambda_2 \times D_2)^{j-i}}{(j-i)!}$. The probabilities of Type I and Type II camera sensors orienting towards the grid point t are expressed as $q_1 = \frac{\alpha_1}{2\pi}$ and $q_2 = \frac{\alpha_2}{2\pi}$, respectively; C_i^h represents the number of combinations of h sensors selected from i Type I sensors, C_{j-i}^{k-h} represents the number of combinations of $k-h$ sensors selected from $j-i$ Type II sensors. For the Type I camera sensor, the detection region $D_1 = \pi{\gamma_1}^2$, and the probability of camera facing towards the center of D_1 is $q_1 = \alpha_1/2\pi$ with density λ_1. The probability of Type II camera facing toward center of $D_2 = \pi{\gamma_2}^2$ is $q_2 = \alpha_2/2\pi$ with density λ_2. Equation (1) can be simplified as follow.

$$\begin{aligned} P(k) &= \sum_{j=k}^{\infty}\sum_{i=0}^{j}\sum_{h=0}^{k} p(i;\lambda_1 \times D_1)C_i^h {q_1}^h(1-q_1)^{i-h} \\ &\quad \times p(j-i;\lambda_2 \times D_2)C_{j-i}^{k-h}{q_2}^{k-h}(1-q_2)^{(j-i-k+h)} \\ &= \frac{1}{k!}e^{-(\lambda_1 D_1 q_1+\lambda_2 D_2 q_2)}(\lambda_1 D_1 q_1+\lambda_2 D_2 q_2)^k \\ &= p(k;\lambda_1 D_1 q_1+\lambda_2 D_2 q_2) \end{aligned} \tag{2}$$

Aiming to the application scenario studied in this paper, a large number of Type I and Type II camera sensors are stochastically deployed in the boundary region Ω of the FoI to be monitored. Due to all heterogeneous camera sensors are randomly located in the boundary region, it is concluded that a grid point in the FoI only has a partial detection region. According to equation (2), for any grid point t in the FoI, it is only needed to calculate the area expectation of the detection region centered at grid point t. Since all heterogeneous camera sensors are not directly deployed in the FoI, it can be seen that the area expectation of the detection region centered at any grid point t in the FoI is approximately equal to the mathematical expectation of effective possible sensing region Φ of any camera sensor in the boundary region Ω. Without loss of generality, we assume $\omega \leq 2\gamma$ so that the entire FoI ψ can be covered by camera sensors located in the boundary region Ω with a high probability. We evaluate the expectation of teffective possible sensing region Φ for two possible cases given in the following.

A. CASE I : $\omega \geq \gamma$

In this case, the width ω of the FoI is larger than or equal to the sensing radius γ of camera sensor. The boundary region Ω is divided into three types of subregions according to the location of camera. Let A_c , A_s and A_n denote the subregions, as illustrated in Fig.5, where, $h = b-\gamma$, if $b \geq \gamma$; otherwise, $h = 0$. Since the effective possible sensing region Φ of camera sensor inside region A_n is equal to zero, we only take analysis of camera sensors located inside A_c and A_s, respectively.

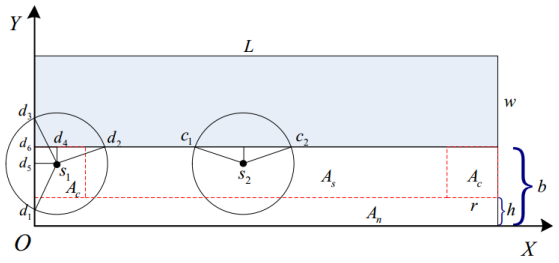

FIGURE 5. Illustration of the effective possible sensing region of a camera sensor located at $s \in \Omega$ with $\omega \geq \gamma$.

1) LOCATION OF CAMERA SENSOR FALLS IN A_C

the effective possible sensing region Φ of the camera sensor (with the camera s_1 in Fig.5) can be expressed as follow.

$$\begin{aligned} \Phi_c(x,y) = \pi\gamma^2 - (\|\Box s_1 d_4 d_6 d_5\| + \|\triangle s_1 d_1 d_5\| + \|\triangle s_1 d_2 d_4\| \\ + \|\widehat{s_1 d_1 d_2}\|) - (\|\widehat{s_1 d_1 d_3}\| - \|\triangle s_1 d_1 d_3\|) \end{aligned} \tag{3}$$

See the Appendix A for the detailed formulas.

2) LOCATION OF CAMERA SENSOR FALLS IN A_S

As illustrated in Fig.5, We observed that the effective possible sensing region for a camera sensor at s_2 can be represented as follow.

$$\begin{aligned} \Phi_s(x,y) &= \|\widehat{s_2 c_1 c_2}\| - \|\triangle s_2 c_1 c_2\| \\ &= \frac{2\arccos\frac{b-y}{\gamma}}{2\pi} \times \pi\gamma^2 - (b-y)\sqrt{\gamma^2-(b-y)^2} \end{aligned} \tag{4}$$

Equations (3) and (4) give the effective possible sensing region of a camera sensor lies at $s = (x, y)$ in the boundary Ω, we take full into account all the possible locations for a camera sensor in the boundary region Ω. Therefore, the expectation of the effective possible sensing region denoted as $E(\Phi)$ for any camera sensor located at $s = (x, y)$ can be obtained by definite integrating equations (3) and (4) over Ω. Thus, $E(\Phi)$ can be expressed as.

$$\begin{aligned} E(\Phi) &= \frac{\iint_{A_c}\Phi_c(x,y)\mathrm{d}A_c + \iint_{A_s}\Phi_s(x,y)\mathrm{d}A_s}{\|\Omega\|} \\ &= \frac{2\int_0^{\gamma}\mathrm{d}x\int_h^b \Phi_c(x,y)\mathrm{d}y + \int_{\gamma}^{L-\gamma}\mathrm{d}x\int_h^b \Phi_s(x,y)\mathrm{d}y}{Lb} \end{aligned} \tag{5}$$

B. CASE II : $\omega < \gamma$

In this case, the width ω of the FoI is smaller than the sensing radius γ of camera sensor. As illustrated in Fig. 6, the boundary region Ω is divided into A_c , A_s and A_n, where, $h = b-\gamma$, if $b \geq \gamma$; otherwise, $h = 0$. Since the effective possible sensing region of camera sensors inside region A_n is equal to zero, we only analyze camera sensors located inside A_c and A_s, respectively.

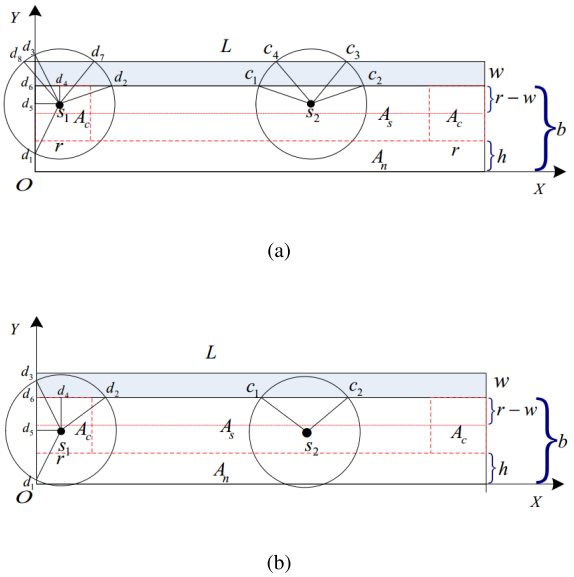

FIGURE 6. Illustration of the effective possible sensing region of a camera sensor located at $s \in \Omega$ with $\omega < \gamma$, (a) $\omega + b - \gamma \le y \le b$, (b) $h \le y \le \omega + b - \gamma$.

1) LOCATION OF CAMERA SENSOR FALLS IN A_c

The effective possible sensing region Φ of the camera sensors (located at s_1 in Fig. 6) can be represented as follow.

$$\Phi_c(x,y) = \begin{cases} \Phi_c^1(x,y) & \omega + b - \gamma \le y \le b \\ \Phi_c^2(x,y) & h \le y \le \omega + b - \gamma \end{cases} \tag{6}$$

Where,

$$\begin{aligned} \Phi_c^1 \approx\ & \pi\gamma^2 - (\|\square\, s_1 d_4 d_6 d_5\| + \|\triangle s_1 d_1 d_5\| + \|\triangle s_1 d_2 d_4\| \\ & + \|\widehat{s_1 d_1 d_2}\|) - (\|\widehat{s_1 d_1 d_3}\| - \|\triangle s_1 d_1 d_3\|) \\ & - (\|\widehat{s_1 d_7 d_8}\| - \|\triangle s_1 d_7 d_8\|) \\ \Phi_c^2 =\ & \pi\gamma^2 - (\|\square\, s_1 d_4 d_6 d_5\| + \|\triangle s_1 d_1 d_5\| + \|\triangle s_1 d_2 d_4\| \\ & + \|\widehat{s_1 d_1 d_2}\|) - (\|\widehat{s_1 d_1 d_3}\| - \|\triangle s_1 d_1 d_3\|) \end{aligned}$$

See the Appendix B for the detailed formulas.

2) LOCATION OF CAMERA SENSOR FALLS IN A_s

As shown in Fig. 6, we can conclude that the effective possible sensing region Φ for camera sensors at s_2 can be represented as follow.

$$\Phi_s(x,y) = \begin{cases} \Phi_s^1(x,y) & \omega + b - \gamma \le y \le b \\ \Phi_s^2(x,y) & h \le y \le \omega + b - \gamma \end{cases} \tag{7}$$

Where,

$$\begin{aligned} \Phi_s^1 &\approx \|\widehat{s_2 c_1 c_2}\| - \|\triangle s_2 c_1 c_2\| - (\|\widehat{s_2 c_3 c_4}\| - \|\triangle s_2 c_3 c_4)\| \\ \Phi_s^2 &= \|\widehat{s_2 c_1 c_2}\| - \|\triangle s_2 c_1 c_2\| \end{aligned}$$

See the Appendix C for the detailed formulas.

Based on the above analysis, the expectation of the effective possible sensing region for a camera sensor can be obtained by definite integrating equations (6) and (7) over Ω, Thus, in this case, $E(\Phi)$ can be expressed as.

$$E(\Phi) = \frac{\iint_{A_c} \Phi_c(x,y)\mathrm{d}A_c + \iint_{A_s} \Phi_s(x,y)\mathrm{d}A_s}{\|\Omega\|} \tag{8}$$

The expectations of the effective possible sensing regions of those two types of heterogeneous camera sensors randomly deployed in the boundary region Ω are denoted as $E(\Phi)_1$ and $E(\Phi)_2$ which can be calculated by equation (5) or (8); $\lambda_1 = \frac{N_1}{\|\psi\|}$ and $\lambda_2 = \frac{N_2}{\|\psi\|}$ denote the sensor density of those two types of heterogeneous camera sensors relative to the FoI ψ; q_1 and q_2 represent the probability of those two types of heterogenous camera sensors facing towards the grid point t in the FoI, respectively. According to equations (2),(5) or (8), the probability of any grid point t in the FoI ψ covered by exactly k heterogeneous camera sensors can be given by

$$\begin{aligned} P(\psi = k) &= p(k; \lambda_1 E(\Phi)_1 q_1 + \lambda_2 E(\Phi)_2 q_2) \\ &= \exp(-(\lambda_1 E(\Phi)_1 q_1 + \lambda_2 E(\Phi)_2 q_2)) \\ &\quad \times \frac{(\lambda_1 E(\Phi)_1 q_1 + \lambda_2 E(\Phi)_2 q_2)^k}{k!} \end{aligned} \tag{9}$$

Lemma 1: Assume that a great number of two heterogeneous camera sensors (Type I and Type II in this paper) are independently and uniformly scattered in the boundary region Ω of the FoI, it is concluded that the k-coverage rate of the FoI can be expressed as

$$\begin{aligned} \mathbb{P} = 1 - \sum_{j=0}^{k-1} & \exp(-(\lambda_1 E(\Phi)_1 q_1 + \lambda_2 E(\Phi)_2 q_2)) \\ & \times \frac{(\lambda_1 E(\Phi)_1 q_1 + \lambda_2 E(\Phi)_2 q_2)^j}{j!} \end{aligned} \tag{10}$$

Proof: Based on the equation (9), we derive that

$$\begin{aligned} \mathbb{P} &= P(\psi \ge k) \\ &= 1 - \sum_{j=0}^{k-1} P(\psi = j) \\ &= 1 - \sum_{j=0}^{k-1} p(j; \lambda_1 E(\Phi)_1 q_1 + \lambda_2 E(\Phi)_2 q_2) \\ &= 1 - \sum_{j=0}^{k-1} \exp(-(\lambda_1 E(\Phi)_1 q_1 + \lambda_2 E(\Phi)_2 q_2)) \\ &\quad \times \frac{(\lambda_1 E(\Phi)_1 q_1 + \lambda_2 E(\Phi)_2 q_2)^j}{j!} \end{aligned}$$

Hence, the *Lemma 1* is proved.

Lemma 2: Assume that $E(\psi \ge k) = \iint_{\psi} \mathbb{P}\mathrm{d}\psi$ denotes the area expectation of the FoI ψ covered by at least k heterogeneous camera sensors. If $E(\psi \ge k)$ is approximately equal to the area of FoI with a high probability, the FoI is said to be approximately complete k-covered.

Proof: Since $E(\psi \ge k)$ is equal to the area of FoI with a high probability, we derive that $E(\psi \ge k) \cong \|\psi\|$. As $E(\psi \ge k) = \iint_{\psi} \mathbb{P}\mathrm{d}\psi = \|\psi\| - \|\psi\| \sum_{i=0}^{k-1} P(\psi = i)$,

we get $E(\psi \geq k) = \|\psi\| - \|\psi\| \sum_{i=0}^{k-1} P(\psi = i) \cong \|\psi\|$, then it is derived that $\|\psi\| \sum_{i=0}^{k-1} P(\psi = i) \cong 0$. Since $\|\psi\| > 0$, we conclude that $\sum_{i=0}^{k-1} P(\psi = i) \cong 0$. From *Lemma 1*, the probability of the FoI which is k-covered is expressed as $\mathbb{P} = 1 - \sum_{i=0}^{k-1} P(\psi = i)$. so we obtain $\mathbb{P} \approx 1$. Thus, according to the *Definition 3*, we know that the *Lemma 2* is proved.

Lemma 3: If other parameters are constant, when the camera sensors randomly deployed in the boundary region Ω are sparse, it is concluded that the k-coverage rate of the FoI is approximately equal to 0.

Proof: when camera sensors are sparsely deployed in the boundary region Ω, it means that $\lambda_1 \to 0$ and $\lambda_2 \to 0$. Due to other parameters are constant, we get $\lim_{\lambda_{1,2}\to 0}(\lambda_1 E(\Phi)_1 q_1 + \lambda_2 E(\Phi)_2 q_2) = 0$, then $\lim_{\lambda_{1,2}\to 0} \exp(-(\lambda_1 E(\Phi)_1 q_1 + \lambda_2 E(\Phi)_2 q_2)) = 1$. Limit the equation (10), we obtain $\lim_{\lambda_{1,2}\to 0} \mathbb{P} = 0$. Thus, the *Lemma 3* is proved.

Lemma 4: If other parameters are constant, when the camera sensors in the boundary region Ω are dense, we conclude that the FoI is approximately complete k covered.

Proof: when camera sensors are densely deployed in the boundary region Ω, we know that $\lambda_1 \to \infty$ and $\lambda_2 \to \infty$. Due to other parameters are constant, we get $\lim_{\lambda_{1,2}\to\infty}(\lambda_1 E(\Phi)_1 q_1 + \lambda_2 E(\Phi)_2 q_2) = \infty$, then $\lim_{\lambda_{1,2}\to\infty} \exp(-(\lambda_1 E(\Phi)_1 q_1 + \lambda_2 E(\Phi)_2 q_2)) = 0$. Limit the equation (10), we obtain $\lim_{\lambda_{1,2}\to\infty} \mathbb{P} = 1$, it means $\mathbb{P} \approx 1$. Thus, the *Lemma 4* is proved.

Example: We take into account such scenario in which a great number of two heterogeneous camera sensors (Type I and Type II camera sensors) are randomly deployed in the boundary Ω of FoI to be monitored. Let $L = 100m, \omega = 60m$, $b = 60m$; the values of γ_1, α_1 and γ_2, α_2 of Type I and Type II camera sensors are $40m$, $\pi/3$ and $60m$, $\pi/2$, respectively. We want to calculate the minimum number of sensors to be scattered in the boundary region Ω so that the FoI ψ is 2-covered width a high probability (0.95 in this example). In order to simplify calculation, we assume the number of Type I is equal to that of Type II. Substituting the values of L, ω, b, γ_1, α_1 and γ_2, α_2 in Lemma 1, we obtain $N_1 = 54$. That means, if we randomly deploy 108 Type I and Type II camera sensors totally in Ω, the FoI ψ is 2-covered with a high probability.

IV. PERFORMANCE EVALUATION

In this section, we use Matlab7.0 to construct simulation scenario to verify the proposed model, it is assumed that all camera sensors are randomly scattered in the boundary region. Besides, the orientations of all camera sensors are also randomly allocated, their value between $[0_o, 360^o]$. A series of simulation experiments are conducted to validate the accuracy of the k-coverage estimation expression for different proportions of heterogeneity corresponding to different parameters in heterogeneous CSNs. In order to obtain more accurate experimental results of simulation scenario, each set of randomized experiments based on different proportions of heterogeneity is repeated 100 times and the mean value is taken as the final experimental result called experimental result.

To simplify these experiments, we set the k-coverage requirement as $k = 1, 2, 3$ .The mainly parameters of scenario are listed in Table 2.

TABLE 2. Mainly scenario parameters.

Parameters	Value
Length of FoI, L	500m
Width of FoI, ω	30m,40m,50m,60m,70m,80m
Width of boundary region, b	30m,40m,50m,60m,70m,80m

A. EFFECT OF CAMERA SENSOR PARAMETERS

We study the effect of three major camera sensor parameters, sensor density, sensing radius, and field of view on the k-coverage rate for different ratios of parameters of Type I and Type II sensors. Let the values of L, ω and b be $500m$, $60m$ and $60m$, respectively.

1) EFFECT OF SENSOR DENSITY

In the first simulation, different numbers of Type I and Type II camera sensors are stochastically deployed in the boundary region of the FoI to study the effect of sensor density on the k-coverage rate where sensing radius $\gamma_1 = 50m$ and $\gamma_2 = 60m$, field of view $\alpha_1 = \pi/3$ and $\alpha_2 = \pi/2$. Fig. 7 indicates the trend of the k-coverage rate as different

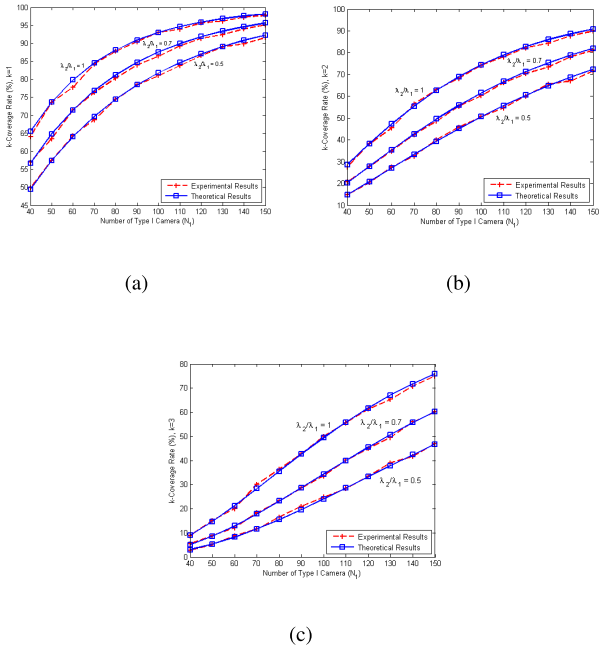

FIGURE 7. Comparison of experimental results and theoretical results corresponding to different number N of camera sensors, (a) $k = 1$, (b) $k = 2$, (c) $k = 3$.

heterogeneity proportions of sensor density $\frac{\lambda_2}{\lambda_1}$ corresponding to scale of Type I camera sensor. It is observed that the k-coverage rate increases as the number of Type I increases due to more camera sensors deployment. When the heterogeneity density ratio $\frac{\lambda_2}{\lambda_1}$ increases, the number of Type II camera sensor increases so that the k-coverage rate increases. The error between theoretical results and experimental results is very small in different numbers of Type I and Type II camera sensors.

2) EFFECT OF SENSING RADIUS

Fixed number of camera sensors are scattered in the boundary region where parameters of Type I $N_1 = 75$, $\alpha_1 = \pi/3$, and Type II $N_2 = 75$, $\alpha_2 = \pi/2$, respectively. Fig. 8 shows the effect of sensing radius of Type I on k-coverage rate for different heterogeneity radius ratios of $\frac{\gamma_2}{\gamma_1}$ corresponding to sensing radius of Type I camera sensor. We observe that the k-coverage rate increases as the sensing radius γ_1 of Type I increases. For a fixed sensing radius γ_1 of Type I, when the ratio $\frac{\gamma_2}{\gamma_1}$ increases, the sensing radius γ_2 of Type II increases so that the k-coverage rate increases.

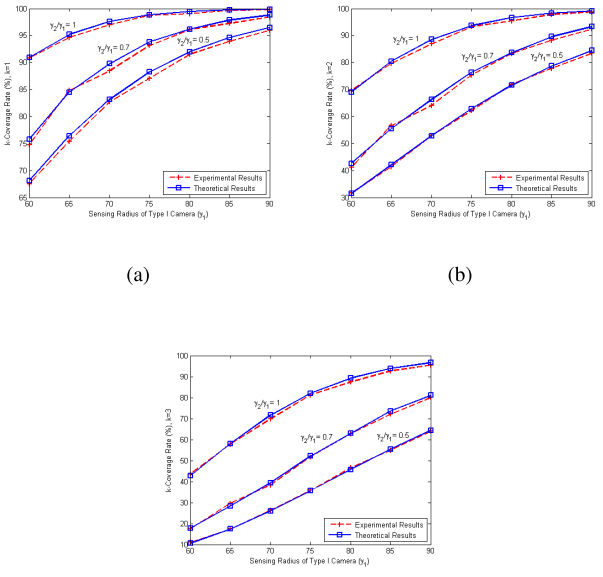

(a) (b)

(c)

FIGURE 8. Comparison of experimental results and theoretical results corresponding to different sensing radius γ of camera sensors, (a) $k = 1$, (b) $k = 2$, (c) $k = 3$.

3) EFFECT OF FIELD-OF-VIEW (FOV)

Fixed number of Type I and Type II camera sensors are randomly deployed in the boundary region. Different values of FoV of Type I camera are selected to show the effect of the FoV on the k-coverage rate where $N_1 = 75$, $\gamma_1 = 50m$ and $N_2 = 75$, $\gamma_2 = 60m$ with Type I and Type II, respectively. As shown in Fig. 9, the k-coverage rate increases as different heterogeneity proportions of FoV $\frac{\alpha_2}{\alpha_1}$ corresponding to FoV

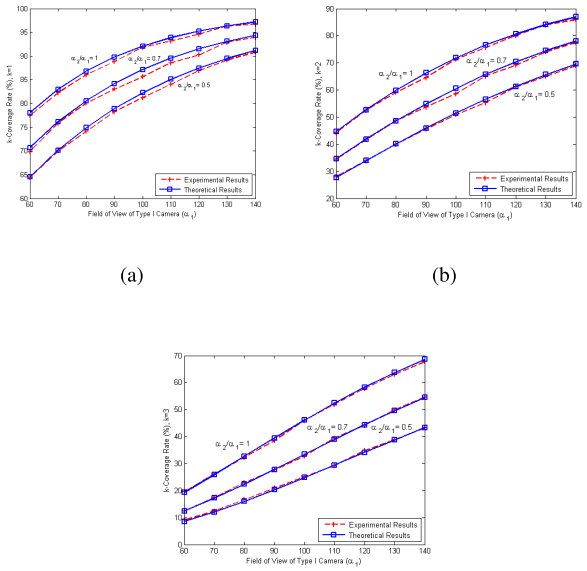

(a) (b)

(c)

FIGURE 9. Comparison of experimental results and theoretical results corresponding to different field of view α of camera sensors, (a) $k = 1$, (b) $k = 2$, (c) $k = 3$.

of Type I camera sensor. We observe that the k-coverage rate increases as the FoV α_1 of Type I increases. When heterogeneity proportions of FoV $\frac{\alpha_2}{\alpha_1}$ increases, the FoV of Type II increases for a fixed α_1 so that the k-coverage rate increases.

B. EFFECT OF WIDTH OF FOI

We study the effect of the width ω of FoI on the k-coverage rate. In this experiment, Let the values of L, b be $500m$ and $60m$, respectively. A large amount of Type I and Type II camera sensors ($N_1 = N_2 = 100$) are randomly deployed in the boundary to monitor the FoI where $\gamma_1 = 50m$, $\alpha_1 = \pi/3$ and $\gamma_2 = 60m$, $\alpha_2 = \pi/2$. Fig.10 shows that the k-coverage

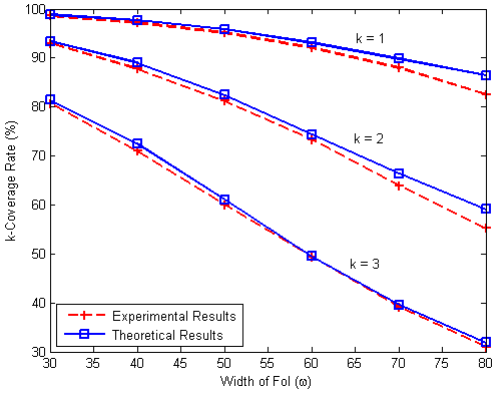

FIGURE 10. Comparison of experimental results and theoretical results corresponding to width ω of the FoI.

rate decreases as the width of FoI increases, this is because that expectation of effective possible sensing region becomes small with increase of the width of FoI. When the width of FoI is larger, the error between experimental results and theoretical results is becoming larger, this is because the k-covered probability of grid points in the horizontal middle of FoI is becoming smaller. However, in the k-coverage estimation expression, the probability of all grid points in FoI k-coverd is equal.

C. EFFECT OF WIDTH OF BOUNDARY REGION

We study the effect of the width b of boundary region on the k-coverage rate. Fixed number of Type I and Type II camera sensors ($N_1 = N_2 = 100$) are stochastically scattered in the boundary region to monitor the FoI, other parameters of Type I and Type II camera sensors are set as $\gamma_1 = 50m$, $\alpha_1 = \pi/3$ and $\gamma_2 = 60m$, $\alpha_2 = \pi/2$. Besides, let the values of L, b be $500m$ and $60m$, respectively. As shown in Fig.11, the k-coverage rate decrease as the width of boundary region increases, this is because that expectation of effective possible sensing region becomes small with increase of the width of boundary region.The error between theoretical results and experimental results is very small in different width of boundary region.

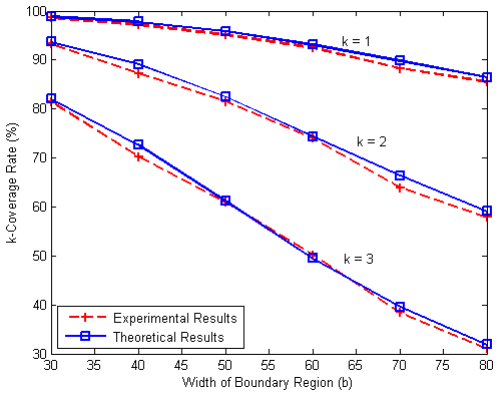

FIGURE 11. Comparison of experimental results and theoretical results corresponding to width b of the Boundary Region.

V. CONCLUSION

In this paper, we studied the k-coverage estimation problem in heterogeneous CSNs with boundary deployment. By assuming that all cameras sensors are stochastically deployed in the boundary region of FoI to achieve monitoring tasks, in order to estimate the minimum number of cameras required for a desired level of k-coverage, we derived a k-coverage estimation expression which reflects the mathematical relationship among sensor density, sensing radius, FoV, width of FoI, width of boundary region and k-coverage. Based on the comparison between experimental results and theoretical results, we demonstrated the correctness of the theoretical k-coverage estimation expression for heterogeneous CSNs with boundary deployment.

APPENDIX A
DETAILED INFORMATION IN EQUATION (2)

All formulas in Equation (2) can be derived from Fig.5

$$\begin{aligned}
\|\square\, s_1d_4d_6d_5\| &= x(b-y)\\
\|\triangle s_1d_1d_5\| &= \frac{x\sqrt{\gamma^2-x^2}}{2}\\
\|\triangle s_1d_2d_4\| &= \frac{(b-y)\sqrt{\gamma^2-(b-y)^2}}{2}\\
\|\widehat{s_1d_1d_2}\| &= \frac{\frac{\pi}{2}+\arcsin\frac{b-y}{\gamma}+\arcsin\frac{x}{\gamma}}{2\pi}\times\pi\gamma^2\\
\|\widehat{s_1d_1d_3}\| &= \frac{2\arccos\frac{x}{\gamma}}{2\pi}\times\pi\gamma^2\\
\|\triangle s_1d_1d_3\| &= x\sqrt{\gamma^2-x^2}.
\end{aligned}$$

APPENDIX B
DETAILED INFORMATION IN EQUATION (5)

All formulas in Equation (5) can be derived from Fig. 6

$$\begin{aligned}
\|\square\, s_1d_4d_6d_5\| &= x(b-y)\\
\|\triangle s_1d_1d_5\| &= \frac{x\sqrt{\gamma^2-x^2}}{2}\\
\|\triangle s_1d_2d_4\| &= \frac{(b-y)\sqrt{\gamma^2-(b-y)^2}}{2}\\
\|\widehat{s_1d_1d_2}\| &= \frac{\frac{\pi}{2}+\arcsin\frac{b-y}{\gamma}+\arcsin\frac{x}{\gamma}}{2\pi}\times\pi\gamma^2\\
\|\widehat{s_1d_1d_3}\| &= \frac{2\arccos\frac{x}{\gamma}}{2\pi}\times\pi\gamma^2\\
\|\triangle s_1d_1d_3\| &= x\sqrt{\gamma^2-x^2}\\
\|\widehat{s_1d_7d_8}\| &= \frac{2\arccos\frac{\omega+b-y}{\gamma}}{2\pi}\times\pi\gamma^2\\
\|\triangle s_1d_7d_8\| &= (\omega+b-y)\sqrt{\gamma^2-(\omega+b-y)^2}.
\end{aligned}$$

APPENDIX C
DETAILED INFORMATION IN EQUATION (6)

All formulas in Equation (6) can be derived from Fig. 6

$$\begin{aligned}
\|\widehat{s_2c_1c_2}\| &= \frac{2\arccos\frac{b-y}{\gamma}}{2\pi}\times\pi\gamma^2\\
\|\triangle s_2c_1c_2\| &= (b-y)\sqrt{\gamma^2-(b-y)^2}\\
\|\widehat{s_2c_3c_4}\| &= \frac{2\arccos\frac{\omega+b-y}{\gamma}}{2\pi}\times\pi\gamma^2\\
\|\triangle s_2c_3c_4)\| &= (\omega+b-y)\sqrt{\gamma^2-(\omega+b-y)^2}.
\end{aligned}$$

REFERENCES

[1] B. Rinner and W. Wolf, "An introduction to distributed smart cameras," *Proc. IEEE*, vol. 96, no. 10, pp. 1565–1575, Oct. 2008.
[2] *Channel Water Monitoring*. Accessed: 2012. [Online]. Available: https://www.ysi.com/applications/ocean-coastal
[3] *Railway Track Monitoring*. Accessed: 2014. [Online]. Available: https://metrom-rail.com/AURA
[4] *Country Border*. Accessed: 2010. [Online]. Available: http://www.ultra-ccs.com/business/surveillance

[5] P.-J. Wan and C.-W. Yi, "Coverage by randomly deployed wireless sensor networks," *IEEE Trans. Inf. Theory*, vol. 52, no. 6, pp. 2658–2669, Jun. 2006.
[6] P. Brass, "Bounds on coverage and target detection capabilities for models of networks of mobile sensors," *ACM Trans. Sensor Netw.*, vol. 3, no. 2, p. 9, 2007.
[7] J.-S. Li and H.-C. Kao, "Distributed k-coverage self-location estimation scheme based on Voronoi diagram," *IET Commun.*, vol. 4, no. 2, pp. 167–177, 2010.
[8] X. Xing, G. Wang, and J. Li, "A square-based coverage and connectivity probability model for WSNs," *Int. J. Sensor Netw.*, vol. 19, nos. 3–4, pp. 161–170, 2015.
[9] J. Zhao and J. C. Zeng, "Sense model and number estimation of wireless multimedia sensor networks," *J. Softw.*, vol. 23, no. 8, pp. 2104–2114, 2012.
[10] Z.-M. Liu, W.-J. Jia, and G.-J. Wang, "Coverage prediction model and number estimation for directional sensor networks," *J. Softw.*, vol. 27, no. 12, pp. 3120–3130, 2016.
[11] M. Karakaya and H. Qi, "Coverage estimation in heterogeneous visual sensor networks," in *Proc. IEEE Int. Conf. Distrib. Comput. Sensor Syst.*, May 2012, pp. 41–49.
[12] Y. Wang and G. Cao, "On full-view coverage in camera sensor networks," in *Proc. IEEE INFOCOM*, Apr. 2011, pp. 1781–1789.
[13] S. He, D.-H. Shin, J. Zhang, J. Chen, and Y. Sun, "Full-view area coverage in camera sensor networks: Dimension reduction and near-optimal solutions," *IEEE Trans. Veh. Technol.*, vol. 65, no. 9, pp. 7448–7461, Sep. 2016.
[14] Z. Yu, F. Yang, J. Teng, A. C. Champion, and D. Xuan, "Local face-view barrier coverage in camera sensor networks," in *Proc. INFOCOM*, Apr./May 2015, pp. 684–692.
[15] Y. Hu, X. Wang, and X. Gan, "Critical sensing range for mobile heterogeneous camera sensor networks," in *Proc. INFOCOM*, Apr./May 2014, pp. 970–978.
[16] X. J. Zhu, J. Li, X. Chen, and M. Zhou, "Minimum cost deployment of heterogeneous directional sensor networks for differentiated target coverage," *IEEE Sensors J.*, vol. 17, no. 15, pp. 4938–4952, Aug. 2017.
[17] T.-Y. Lin, H. A. Santoso, K.-R. Wu, and G.-L. Wang, "Enhanced deployment algorithms for heterogeneous directional mobile sensors in a bounded monitoring area," *IEEE Trans. Mobile Comput.*, vol. 16, no. 3, pp. 744–758, Mar. 2017.
[18] Y. Wang, F. Li, and F. Fang, "Poisson versus Gaussian distribution for object tracking in wireless sensor networks," in *Proc. 2nd Int. Workshop Intell. Syst. Appl.*, May 2010, pp. 1–7.

ZHIMIN LIU was born in Chenzhou, China. He received the B.E. degree from Northeastern University in 2006 and the M.E. degree from South China Agricultural University in 2010, and the Ph.D. degree from the School of Information Science and Engineering, Central South University, in 2017. He is currently an Assistant with the College of Computer and Information Engineering, Hunan University of Commerce. His current research interests include wireless multimedia sensor network, sensor-cloud, and privacy protection.

ZHANGDONG OUYANG was born in Chenzhou, China. He received the B.E. degree from the Hunan University of Arts and Science in 2005, and the M.E. and Ph.D. degrees from Hunan Normal University in 2008 and 2011, respectively. He is currently an Associate Professor with the School of Mathematics and Computational Science, Hunan First Normal University. His research interests include topological graph theory, graph theory algorithm, and complex network.